THE JOURNAL OF PHYSICAL CHEMISTRY B

Article

pubs.acs.org/JPCB

Mechanism of Fast Pyrolysis of Lignin: Studying Model Compounds

Victoria B. F. Custodis,[†] Patrick Hemberger,[‡] Zhiqiang Ma,[†] and Jeroen A. van Bokhoven*[,†,§]

[†]Department of Chemistry and Applied Biosciences, Institute for Chemical and Bioengineering, ETH Zurich, HCI E 127, Vladimir-Prelog-Weg 1, 8093 Zurich, Switzerland

[‡]Molecular Dynamics Group, Paul Scherrer Institute, CH-5232 Villigen-PSI, Switzerland

[§]Laboratory for Catalysis and Sustainable Chemistry, Paul Scherrer Institute, WLGA 135, 5232 Villigen, Switzerland

Supporting Information

ABSTRACT: Fast pyrolysis of lignin is one of the most promising methods to convert the complex and irregular structure of lignin into renewable chemicals and fuel. During pyrolysis the complex set of radical reactions, rearrangements, and eliminations is influenced by temperature, pressure, and the lignin origin and structure. This model compound study aims to understand reaction pathways and how primary intermediates lead to the observed product selectivity. The pyrolysis microreactor directly connected to the gas chromatograph with a mass spectrometer (py-GC/MS) detects the final products, while imaging photoelectron photoion coincidence (iPEPICO) with VUV synchrotron radiation shows primary decomposition radicals. The tested model compounds, diphenylether (DPE) and ortho-methoxyphenol (guaiacol), represent a common lignin linkage and the most present subunit in lignin, respectively. Radical fragments, such as the hydroxycyclopentadienyl radical in guaiacol decomposition, are identified by mass-selected threshold photoelectron spectra (ms-TPES) in excellent agreement with the Franck−Condon simulation. While homolysis produces phenoxy-, phenyl-, and hydroxyphenoxy radicals, which are observed in high vacuum, radically initiated reactions are dominant in ambient conditions and produce recombination and rearrangement products, such as 2-hydroxybenzaldehyde in the case of guaiacol. The degree of substitution plays a dominant role in both the stabilization of the intermediate radical and the following degree of recombination. The recombination of phenoxy radicals is enhanced compared to hydroxy-phenoxy radicals.

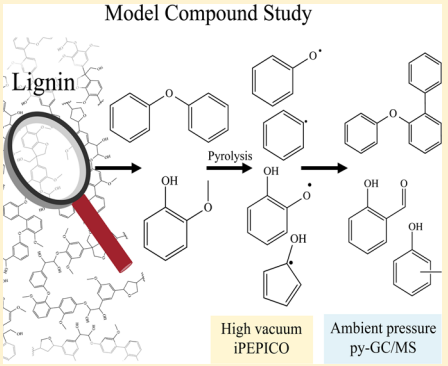

INTRODUCTION

When looking for sustainable alternatives for fuel and chemicals, lignin as the third most common biopolymer gains in importance. Biomass is an inexpensive source consisting of three main components: cellulose, hemicellulose, and lignin. Lignin accounts for 15−30% by weight and 40% by energy.[1] It has a high potential as a feedstock for bulk and fine chemicals, especially aromatic compounds.[2,3] Lignin is an irregular macromolecule built from different phenolic monomers.[4] The most promising method to depolymerize the lignin structure to get valuable chemicals ready for further treatment is pyrolysis, fast pyrolysis in particular.[5] Fast pyrolysis yields a mixture of mostly oxygen containing compounds called bio-oil. A lot of research has been done to improve the yield and quality of products and to reduce char formation.[5−10] However, the mechanistic considerations of depolymerization during pyrolysis have received relatively little attention. Thermal-induced decomposition of macromolecules results from radical formation, which can easily recombine and eventually form undesired char. Due to its complexity and irregularity, the lignin structure is often represented by model compounds, such as phenylphenethyl ether,[11,12] diphenylether (DPE), phenol,[13,14] vanillin, anisole, guaiacol, dimethoxyphenol, and isoeugenol.[15,16] These model compounds either represent an often occurring lignin bonding, a building block, or a component of the pyrolysis oil.[12,17] Phenylphenethyl ether (PPE), for example, is a model compound mimicking the β-O-4 bond. Its decomposition mechanism depends highly on the temperature. Extensive studies have shown that there are two dominating concerted mechanisms, 6-centered retro-ene and Maccoll elimination,[18,19] which lead both to phenol and styrene as end products.[20,21] The retro-ene mechanism first forms styrene and 2,4-cyclohexadiene-1-one, which isomerizes to phenol.[22] Phenol, as a simplified model compound, forms cyclopentadienyl radicals by decarbonylation after its phenoxy radical formation.[12,14,17]

While PPE has been studied extensively, DPE, as a model for the aromatic ether bond, has not yet been in focus of studies concerning lignin pyrolysis.[23,24] The expected thermal decomposition into phenol and benzene is completely unrelated to the elimination mechanisms competing in the β-O-4 model. Additional further reactions of simple phenoxy- and phenyl-radicals may be observable. Guaiacol is tested in this study to exemplify the influence of methoxy-groups onto the model

Received: April 14, 2014
Revised: June 15, 2014

   dx.doi.org/10.1021/jp5036579 | J. Phys. Chem. B XXXX, XXX, XXX−XXX

compound.[25] The methoxy-phenol-subunit makes up to 50−95% of the lignin macromolecule.[26]

Here, we employ two types of pyrolysis setups, which are able to detect isolated radicals as well as stable end products. In the py-GC/MS-setup, reactants have a relatively long residence time until separation and analysis. Only products after decomposition, rearrangement, recombination, and stabilization are detected, since reactive intermediates, such as radicals and carbenes, do not survive their transport from generation to detection. To understand the decomposition of lignin model compounds in the first few hundred microseconds we applied high vacuum pyrolysis in a tubular reactor in a molecular beam, which enables the detection of elusive species and determine the unimolecular decomposition mechanism under reactive collision-reduced conditions. The decomposition products are ionized by VUV synchrotron radiation and detected in an imaging photoelectron photoion coincidence (iPEPICO) setup, which allows recording mass-selected threshold photoelectron spectra (ms-TPS), serving as an isomer-selective detection tool.[27,28]

The direct comparison of high vacuum pyrolysis and pyrolysis at ambient pressure is a suitable strategy to study and understand the formation of intermediates and their stabilization.[29] We believe that new insights are gained showing the different behavior of the tested model compounds. Relating the isolated primary decomposition products to stable end products is a key step in understanding lignin depolymerization. Once the decomposition pattern is identified, it can be influenced and lignin depolymerization can be tuned accordingly.

EXPERIMENTAL SECTION

Materials. As starting materials we studied: diphenylether (>99.5%, Aldrich), *ortho*-methoxyphenol/guaiacol (>99%, Fischer Scientific). All quartz devices have been calcined before reaction in air at 550 °C for 5 h with a heating rate of 5 °C/min.

iPEPICO Experiment and VUV-Beamline. To investigate the primary thermal decomposition mechanism pyrolysis of guaiacol and DPE has been performed in the imaging photoelectron photoion coincidence (iPEPICO) endstation[30,31] of the VUV-Beamline at the Swiss Light Source, which both are only briefly described here.[32] The X04DB bending magnet provides the synchrotron radiation, which is collimated by a toroidal mirror onto a 150 or 600 L/mm grating, dispersed and focused by another mirror onto the exit slits, located in the gasfilter running with a mixture of argon (30 mol %), neon (60 mol %), and krypton (10 mol %). The latter one suppresses the high-order radiation also diffracted by the grating. The photon-energy resolution is typically around 5−12 meV as measured by the 11s' Rydberg state of argon. The pyrolysis setup consists of a resistively heated SiC-tube (1 mm i.d./2 mm o.d., 10 mm heated zone), through which an argon gas stream is expanded carrying the starting material (dilution = 0.01%). A typical backing pressure of 300 mbar has been applied onto the 100 μm nozzle (upstream of the reactor) to generate a molecular beam, which enters the source chamber (10^{-4} mbar) of the iPEPICO endstation. The molecular beam is skimmed (2 mm Beam Dynamics Inc. skimmer), enters the spectrometer chamber [$(1-5) \times 10^{-6}$ mbar] and is subsequently ionized by VUV light. Electrons are extracted in a 120 V/cm field velocity focused in a VMI spectrometer and detected on a Roentdek DLD40 position sensitive detector. Ions are accelerated in the opposite direction and detected in a Jordan TOF (C-726) mass spectrometer, and the ionization events are correlated in real-time in a multiple start−multiple stop scheme.[33] For the identification of isomers and intermediates, mass-selected threshold photoelectron spectra have been recorded with a resolution of 5−12 meV. The hot electron background has been subtracted, applying the method from Sztaray and Baer.[34] It is possible to directly detect temperature-dependent radicals and intermediates, which have been identified by their specific ionization energies and vibrational fingerprint as measured by the ms-TPES. The temperature is measured at the reactor surface by means of a type-c thermocouple, having an accuracy of roughly ±100 K, due to imperfect contact with the surface. The residence time in the reactor is estimated to be several hundred microseconds. Mass spectra scans (Figure 2) were taken at different temperatures.

Py-GC/MS. Pyrolysis of the model compounds has been performed in a platinum coil pyrolyzer (5150, CDS Analytical) with an open-ended quartz reactor (i.d. = 2.0 mm, o.d. = 2.5 mm, length = 2.5 cm, approximate heating capacity = 0.073 J/K) packed with loose quartz wool in a helium carrier gas stream. 1−2 μL of model compound has been pyrolyzed at a heating rate of 20 °C/ms and then held at the end-temperature for 1 min. The pyroprobe is resistively heated by a calibrated rod and its temperature simultaneously monitored. Temperature of the interface and the transfer line is also observed at several points.

The pyrolysis products are directly injected into an Agilent 7890A GC with Agilent 5975C MS system through the interface and transfer line at 300 °C. The GC is equipped with a thermal conductivity detector (TCD), which has been calibrated for the most abundant non condensable products. The condensable fraction injected into the GC/MS system has been characterized by peak identification according to the NIST08 mass spectrum library. The stated selectivity is based on the peak area each product divided by the overall peak area of the products and the conversion is calculated by using the integrated peak area, which has been calibrated for each model compound. All reactions have been at least performed in duplicate and reproduced within 95%.

Gaussian Calculations. Gaussian 09 has been utilized, applying the B3LYP functional and the 6-311++G(d,p) basis set to calculate the equilibrium geometry and force constant matrixes,[35a] which are used to compute Franck−Condon factors with the program ezSpectrum.OSX.[35b] Reliable ionization energies and relative energies are calculated applying the CBS-QB3 method.[36,37]

RESULTS

Figure 1 shows the product distribution of ambient pressure pyrolysis in the py-GC/MS-setup of (a) DPE and (c) guaiacol. Conversion (dotted line) of DPE starts above 650 °C, yielding a major fraction of recombination products (Figure 1b) with a molar mass higher than the starting compound. Additional products are benzene (D-7) and dibenzofuran (m/z = 168, molecule D-6 in Figure S3 of the Supporting Information). In the following section, the molecules are labeled according to their molecule of origin and listed in Figure S3 of the Supporting Information. With increasing temperature, the reactivity to biphenyl (D-8), benzene (D-7), and dibenzofuran (D-6) increases and fewer recombination products are detected. A minimum of these is observed at 800 °C, while

dx.doi.org/10.1021/jp5036579 | J. Phys. Chem. B XXXX, XXX, XXX−XXX

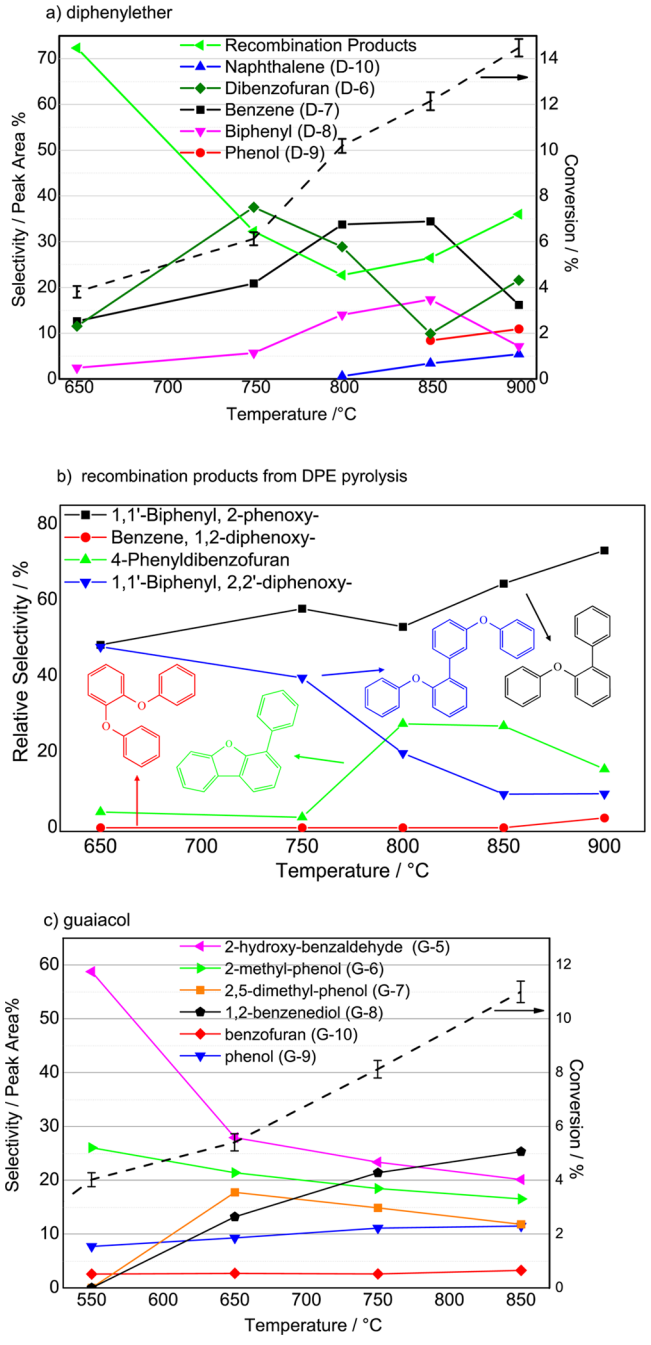

Figure 1. Selectivity as a function of temperature of the ambient pressure pyrolysis (colored lines) and the conversion (dashed line) of (a) diphenylether, (b) a detailed description of the recombination products, and (c) guaiacol in the pyroprobe-reactor.

the recombination product comprising two DPE molecules (2,2′-diphenoxy-1,1′-biphenyl) decreases steadily. At slightly lower temperature maximum selectivity of benzene (D-7) and biphenyl (D-8) is reached. At higher temperatures (>800 °C) recombination products of D-6 are observed (Figure 1b). Only above 850 °C do phenol (D-9) and naphthalene (D-10) appear as reaction products. Conversion of DPE is about 15% at 850 °C. Carbon monoxide is observed in trace amounts (~0.1−0.4 wt %) above 800 °C. Above these temperatures D-10 and trace amounts of compounds comprising fractions from aromatic rings, such as styrene and indene, are detected, but no five-ring compounds, unlike in the iPEPICO experiment (vide infra). Guaiacol conversion starts at 550 °C and increases up to 11% at 850 °C. First, 2-hydroxybenzaldehyde (G-5) is formed together with methylphenol (G-6), phenol (D/G-9), methoxybenzene, and benzofuran (G-10). With increasing temperature, the selectivity to 2,5-dimethylphenol (G-7) and 1,2-benzenediol (G-8) (catechol) increases, while the selectivity to 2-hydroxybenzaldehyde (G-5) strongly decreases. At high temperature more 1,2-benzenediol (G-8) is formed and the phenol concentration is increasing steadily. Benzofuran (G-10), dihydrobenzofuran, toluene, and methoxybenzene are detected in trace amounts.

Figure 2 shows the normalized mass spectra at different temperatures of (a) DPE and (b) guaiacol in the iPEPICO experiment in high vacuum. The collision-reduced conditions in high vacuum facilitate detection of primary decomposition products and radicals. Each intermediate and product has been identified by its specific ionization potential according to its ms-TPES. A table listing all measured ionization potentials and the literature values is provided in the Supporting Information. The lignin model compound for the aromatic ether bond shows first decomposition products at a 610 °C reactor temperature. Compounds with the masses m/z = 65 and 66 are emerging first together with m/z = 77, 78, 93 and 94, which are identified as cyclopentadienyl radical (D-3), cyclopentadiene, phenyl radical (D-1), benzene (D-7), phenoxy radical (D-2), and phenol (D-9) respectively. The phenoxy radical (D-2) and phenol (D-9) show only little signal intensity. The species appearing at m/z = 142 at intermediate pyrolysis temperature possesses a broad asymmetric peak shape in the TOF spectrum, which suggests that it is formed in a dissociative ionization process. Since the dissociating ion stays one-third of its TOF (several microseconds) in the acceleration stage of the mass spectrometer, ionic dissociations with rates in the range of 10^3–10^7 s^{-1} result in asymmetric peak shapes and can thus be distinguished from pyrolysis products formed in the tubular reactor. Dissociative ionization of DPE occurs at room temperature at 11.6 eV (see breakdown diagram, Figure S2 of the Supporting Information, effusive inlet system), but since sufficient internal energy is deposited in the neutral molecule at intermediate pyrolysis temperatures, this onset can be shifted toward lower photon energies (see Figure 2a).[38−40] In some mass spectra, especially when the dilution of DPE in the carrier gas was on the order of 5−10%, we observed bimolecular reactions to a higher extent. In this case, we could identify m/z = 142 to three isomers of the composition $C_{10}H_{11}$ (see the Supporting Information for more details); however, these features are not observed at the high dilution used to generate Figure 2a (0.01%). Above the 730 °C reactor temperature, smaller amounts of dibenzofuran (m/z = 168, D-6) are detected. At higher temperatures, above 900 °C, many different compounds and radicals are produced comprising further decomposition fragments, such as benzyne (m/z = 76), propargyl radical (D-4, m/z = 39), acetylene (D-5, m/z = 26; not visible at 10 eV photon energy), and 1,3-butadiyne (m/z = 50). In other measurements of DPE with a dilution of 5−10%, the relative signal intensities of D-6 and that of m/z = 142 increased and different recombination products, such as the indenyl radical, styrene, and naphthalene (D-10), have been detected.

Guaiacol (Figure 2b) shows the first signs of fragmentation at 500 °C with signals at m/z = 110, 109, and 108, simultaneously, with m/z = 15, the methyl radical. The compounds with m/z = 109, 110, and 108 are assigned to *o*-hydroxy-phenoxy radical

dx.doi.org/10.1021/jp5036579 | J. Phys. Chem. B XXXX, XXX, XXX−XXX

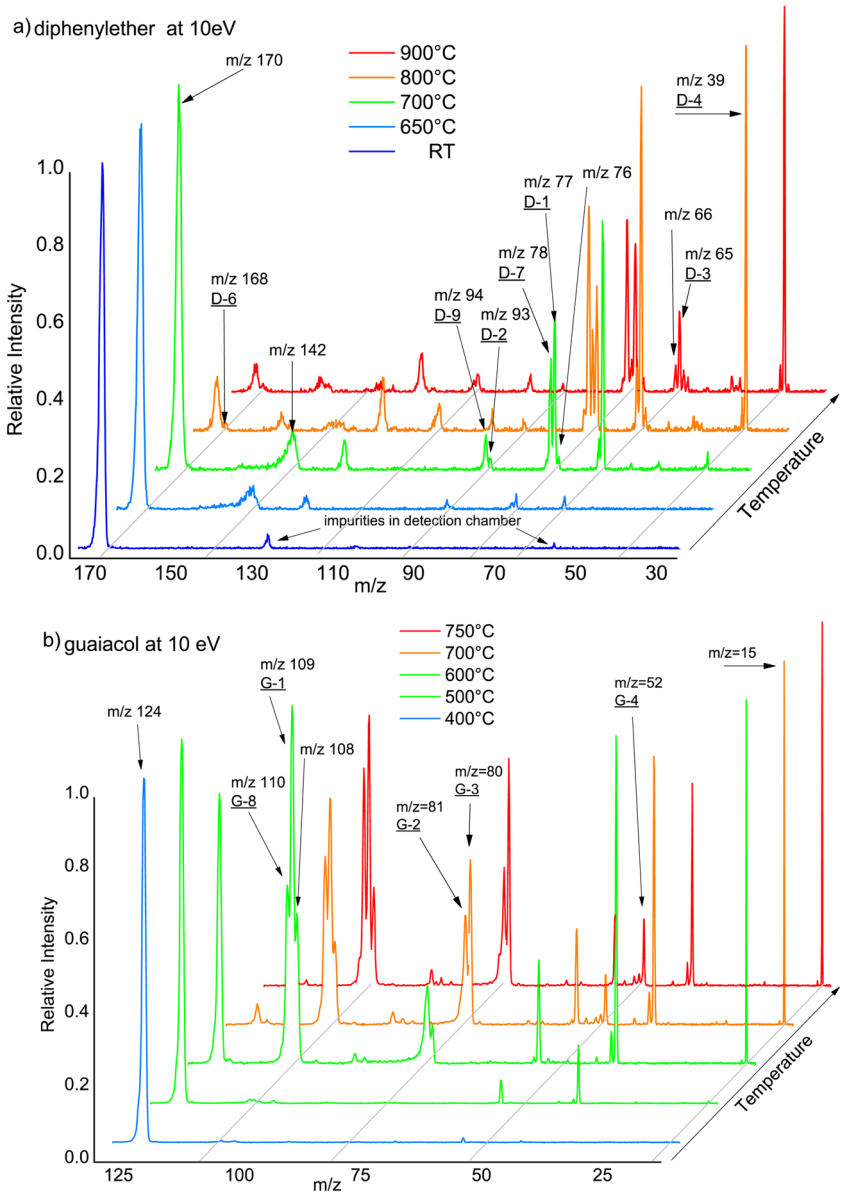

Figure 2. TOF-MS scans of (a) diphenylether and (b) guaiacol pyrolysis at different temperatures at 10 eV photon energy.

(G-1) and its stabilized forms 1,2-benzenediol (G-8) and 6-hydroxycyclohexy-2,4-dien-1-one, respectively. At 600 °C, the reactor temperature m/z = 80 and 81 is detected and at even higher temperature m/z = 52, which is identified as 1-buten-3-yne. The compounds with m/z = 80 and 81 are assigned as 2,4-cyclopentadien-1-one (G-3, IE: 9.40 eV) and the hydroxycyclopentadienyl radical (G-2, IE: 7.48 eV), respectively. A ms-TPES of this radical is depicted in Figure 3, showing an excellent agreement with a Franck−Condon simulation and thus confirming its appearance as an intermediate in this unimolecular reaction.

At high temperature, similar to the results of DPE, there are various fragments and recombination products, such as propargyl radical (D-4, m/z = 39) and smaller amounts of fulvene (m/z = 78). The signal of m/z = 110 is 1,2-benzenediol (G-8), and also trace amounts of phenol (G-9, m/z = 94) are visible, indicating bimolecular reactions. In summary, our results on the decomposition of guaiacol confirm the findings of Scheer et al.[25] Almost full conversion is already achieved at around 700 °C, which is a few hundred K lower compared to Scheer et al.[25] We attribute this observation to the used seeding gas, argon, and different reactor conditions like backing pressure, flow rates, and continuous vs pulsed molecular beam. Additionally, hot and sequence band transitions appearing in the measured ms-TPE spectra indicate the less efficient cooling of the intermediates at the outlet of reactor, which is in accord with literature findings.[41] This can come along with the reduced backing pressure (100 mbar) under continuous conditions (vs 2600 mbar pulsed), and the decrease of the pressure by another 150 μm pinhole at the entrance of the reactor used in this study. The effective pressure at the inlet is therefore lower compared to the pulsed beam, resulting in a lower pressure drop and thus to a less efficient cooling, slower molecular beam and longer residence times.

DISCUSSION

The aim of this study is to compare the primary decomposition products detected in the iPEPICO experiment with the stabilized end products in py-GC/MS to get a deeper

dx.doi.org/10.1021/jp5036579 | J. Phys. Chem. B XXXX, XXX, XXX−XXX

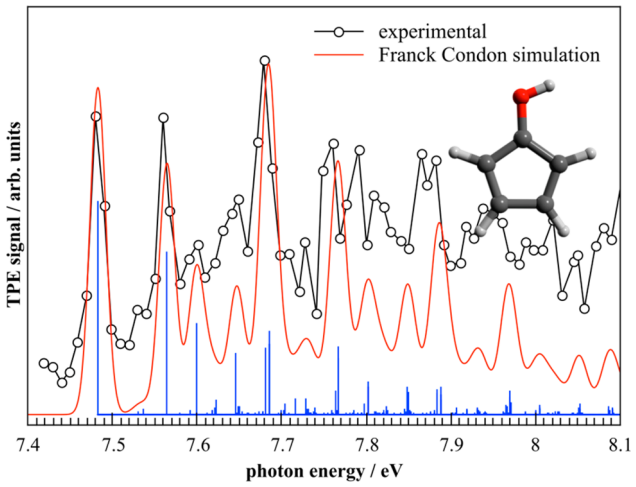

Figure 3. ms-TPE spectrum of hydroxycyoclopentadienyl radical. Excellent agreement with Franck−Condon simulation confirms the assignment.

understanding of the crucial reactions taking place upon pyrolysis of lignin. DPE, the model-compound for diaryl ether structures in lignin, shows different products in both experimental setups. At ambient pressure, there are more than 50% (by peak area) recombination products building from diphenylether-, phenoxy-, and phenyl radicals. Some of the recombination products are shown in Figure 4 and their relative selectivity is shown in Figure 1b. They prove the presence of the phenyl radical (D-1) and the phenoxy radical (D-2) in the reaction zone, which can directly be compared to the initiation step found in high vacuum pyrolysis conditions, the homolysis of the C−O bond.[42] The resulting phenyl and phenoxy radicals are observed together with the cyclopentadiene and cyclopentadienyl radical (D-3). D-2 (m/z = 93) shows relatively small signal intensity, indicating a small stability at elevated temperatures. From single molecule decomposition of phenol and anisole, it is known that D-2 (m/z = 93) is highly unstable and readily decomposes to a cyclopentadienyl radical and carbon monoxide.[14,43,44] There are, however, no five-ring compounds observed in ambient conditions (py-GC/MS) and only trace amounts of carbon monoxide, which could prove this further unimolecular decomposition. Instead, D-2 would recombine readily with other radicals, which is observed (see Figure 4).

Dibenzofuran (D-6) is only observed in trace amounts at higher temperatures in the iPEPICO setup, but its relative selectivity increases with higher DPE concentration (at the iPEPICO experiment, not shown) and temperature in both experimental setups. Its formation represents a different, concerted route to the homolytic ether bond dissociation but is of minor relevance under high vacuum conditions.[42,45] Due to the fact that its relative abundance decreases with the DPE dilution, it must be initiated by bimolecular interactions.

The observed products of guaiacol pyrolysis in both experimental setups (Figure 5) do not show the obvious similarities already observed with DPE. The unimolecular decomposition of guaiacol consists of demethylation, resulting in an *o*-hydroxy-phenoxy radical (G-1, m/z = 109). At higher temperatures, the product of decarbonylation is observed yielding the hydroxycyclopentadienyl radical (G-2, m/z = 81). Scheer et al.[25] studied the guaiacol decomposition with matrix isolation infrared spectroscopy and photoionization mass spectrometry. They found a very similar decomposition pathway with 1-buten-3-yne (G-4) as the end product. They report that G-2 (m/z = 81) eliminates one H atom to form 2,4-cyclopentadien-1-one (G-3), which steps in at higher temperatures (Figure 2b). The hydroxycyclopentadienyl radical (G-2) could be identified in our setup by its adiabatic ionization potential of IE_{ad} = 7.48 eV (see Figure 3), which compares well with a calculated one of 7.54 eV (CBS-QB3). At ambient conditions, however, first 2-hydroxybenzaldehyde (G-5) is

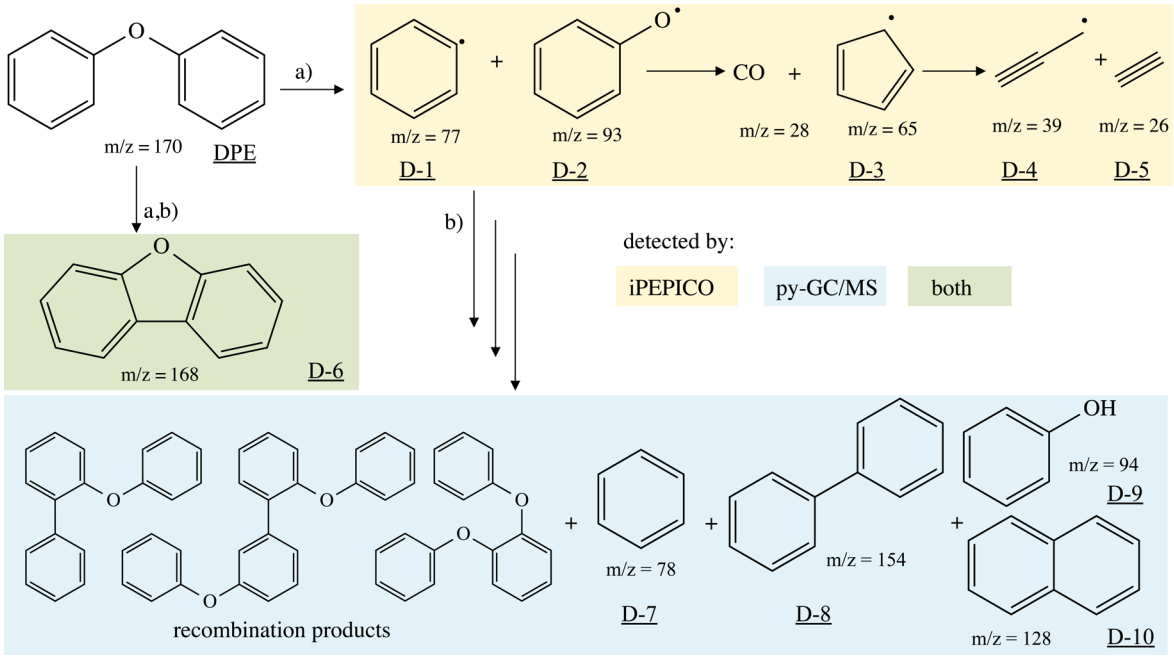

Figure 4. Overview reaction mechanism and detected products of pyrolysis in (a) iPEPICO (high vacuum) and (b) py-GC/MS (ambient pressure). The molecules are labeled according to the model compound (D for DPE).

dx.doi.org/10.1021/jp5036579 | J. Phys. Chem. B XXXX, XXX, XXX−XXX

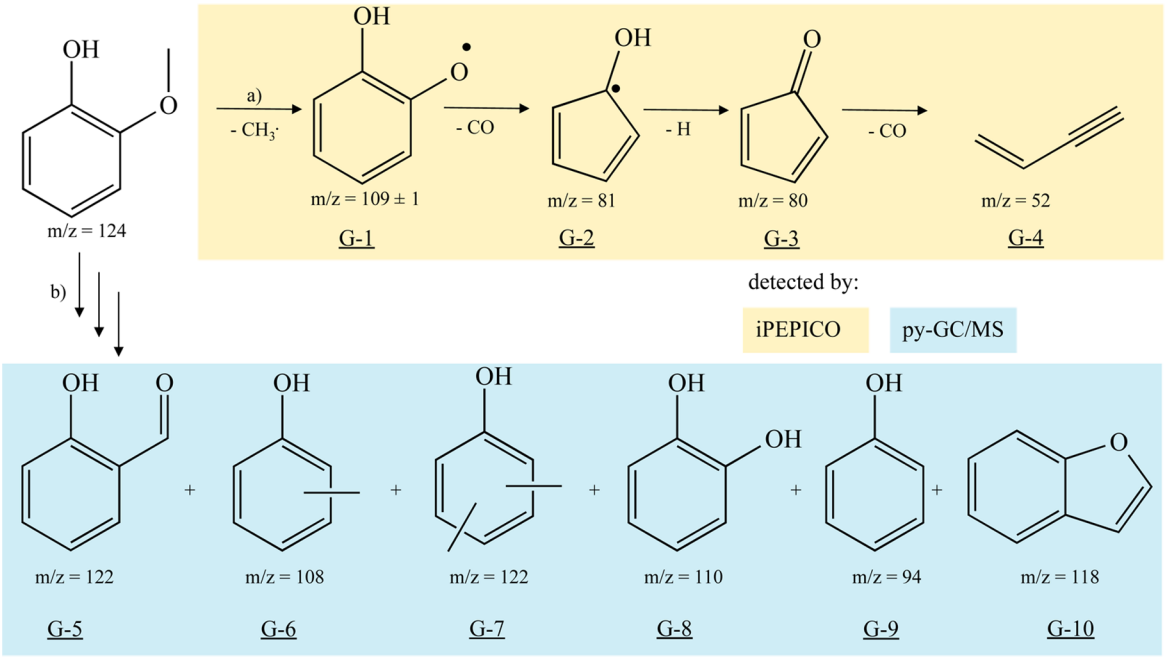

Figure 5. Reaction mechanism and detected products of guaiacol pyrolysis in (a) iPEPICO (high vacuum) and (b) py-GC/MS (ambient pressure). The molecules are labeled according to the model compound (G for guaiacol). A detailed list is found in Figure S3 of the Supporting Information.

formed together with methylated phenols (G-6 and G-7). Only at high temperatures, 1,2-benzenediol (G-8) is formed, which represents the stabilized product of G-1 detected in the iPEPICO experiment.

The (methylated) phenolic compounds (G-6 and G-7) make almost up to 50% of the total detected products (by peak area) in the py-GC/MS setup and cannot result directly from G-1. One possible mechanism suggested is the phenol formation by recombination of a G-2 with a methyl radical.[25] This would also explain the lack of five-ring species detected by py-GC/MS. Another explanation for the high level of phenol formation is the decarbonylation of the formed 2-hydroxybenzaldehyde (G-5) (see decreasing in Figure 1b). Therefore, the formed phenolic radicals would not undergo further unimolecular decarbonylation to form cyclopentadienone species.[25]

G-5 is formed in a different reaction route than homolysis of the methoxy group: via hydrogen abstraction, the guaiacol forms a corresponding radical, which readily undergoes 1,2-aryl-shift followed by another hydrogen abstraction.[45,46] The formation of G-5 requires a high radical concentration in the reaction zone, since two hydrogen abstractions by radicals are necessary. The product formation of methyl-phenols (G-6 and G-7) and phenol (G-9) itself, which are produced at higher temperatures, require even more radical interactions. Therefore, this route is radical initiated and bases highly on bimolecular interactions. Both reaction routes, radical initiated and homolytic, are generally in good agreement with other studies of model compounds.[15,25,29,47]

With regards to the general product selectivity at the different temperatures, there are similarities to the typical selectivity patterns observed at pyrolysis of lignin. With increasing temperature, less-substituted phenols are detected and the selectivity for alkoxy phenols decreases while the selectivity for aromatic hydrocarbon (including naphthalene) increases.[7]

At ambient pressure, DPE forms detectable products with molecular weight above 300−400 m/z. With increasing temperature, the selectivity for large recombination products decreases and recombination products of D-6 emerge. Interestingly, the phenoxy- and phenyl radicals (D-1 and D-2 especially phenoxy radicals) show a high tendency to recombine, while the hydroxy-phenoxy radical (G-1) does not. Brigati et al. determined the relative stabilites of substituted phenoxy radicals, according to their bond dissociation enthalpies, and they concluded that methoxy substituents increase the radical stability.[48] The radical stability seems to determine the degree of recombination compared to that of internal rearrangement.

Earlier studies have also shown that the present radical concentration in lignin influences not only the rate of decomposition and recombination but also the product distribution and selectivity.[15,16,34] The degree of substitution on the phenolic subunits in lignin will be decisive for the stability of the corresponding radical[48−50] and thus the degree of recombination and char formation during lignin pyrolysis. Therefore, not only the yield but also the selectivity is very dependent on the stabilization of the primary radicals and their distinct initiation, but further studies concentrating on the dependence of radical stability and the resulting product selectivity are needed. This also partially explains the major differences in yield and selectivity of different lignin samples of different biological origin and of different separation methods. For example, hardwood based lignin contains much more syringol units than softwood based lignin, which mainly consists of guaiacol-related compounds.[51] This study focuses on one typical lignin bond, the aromatic ether bond, which cannot undergo any other elimination reactions and decomposes at different temperatures than the β-O-4 bond. The studied 4-O-5 bond may not be as frequent and present as the β-O-4 bond, but its decomposition intermediates are also representative for other frequent lignin linkages. At higher temperatures, the 5−5′-bond between two aromatic structures breaks[52] but results in similar (phenyl-) radicals, as observed in the case of DPE.

dx.doi.org/10.1021/jp5036579 | J. Phys. Chem. B XXXX, XXX, XXX−XXX

CONCLUSION

Both guaiacol and DPE have been studied in the pyrolysis-GC/MS and high vacuum pyrolysis in the iPEPICO setup located at the VUV beamline of the Swiss Light Source. By comparing the decomposition mechanism measured under collision-reduced conditions in high vacuum with the products formed in ambient pressure pyrolysis, two main decomposition routes have been identified: first, the homolytic fission of the weakest bond-forming radicals and, second, the radical initiation leading to different radicals, which further rearrange and recombine. The most relevant reaction step in lignin pyrolysis is therefore the primary radical formation, which then initiates further reactions we observe at ambient conditions. There is a lack of high molecular weight recombination products in guaiacol pyrolysis. Recombination of phenoxy and phenyl radicals is enhanced compared to that of methoxy-substitued radicals. Mass-selected threshold photoelectron spectra (ms-TPES) of the model compound pyrolysis enabled us to determine these primary decomposition products precisely and thus relate their stabilities. If stabilization of these primary intermediates in lignin were possible, the product selectivity of lignin could be tuned toward much more desired sustainable chemicals.

ASSOCIATED CONTENT

Supporting Information

The discussion and determination of the compound with m/z = 142, measured ionization potentials for all the observed compounds, the overview of the most relevant observed species with the used labeling, and the breakdown diagram of dephenylether. This material is available free of charge via the Internet at http://pubs.acs.org.

AUTHOR INFORMATION

Corresponding Author

*E-mail: jeroen.vanbokhoven@chem.ethz.ch. Tel: +41 44 632 5542.

Notes

The authors declare no competing financial interest.

ACKNOWLEDGMENTS

The authors thank Swiss National Science Foundation for the finical support (NRP66, no. 406640-136892). The experiments were performed at the VUV beamline of the Swiss Light Source, located at the Paul Scherrer Institute (PSI). The work was financially supported by the Swiss Federal Office for Energy (BFE Contract Number 101969/152433). Calculations were performed at the HPC cluster Merlin4 (PSI).

REFERENCES

(1) Zakzeski, J.; Bruijnincx, P. C. A; Jongerius, A. L.; Weckhuysen, B. M. The Catalytic Valorization of Lignin for the Production of Renewable Chemicals. *Chem. Rev.* **2010**, *110*, 3552−3599.
(2) Bridgwater, A. V. Review of Fast Pyrolysis of Biomass and Product Upgrading. *Biomass Bioenergy* **2012**, *38*, 68−94.
(3) Dickerson, T.; Soria, J. Catalytic Fast Pyrolysis: A Review. *Energies* **2013**, *6*, 514−538.
(4) Freudenberg, K.; Richtzenhain, H.; Flickinger, E.; Engler, K. Modellversuche zur Ligninfrage. *Angew. Chem.* **1939**, *9*, 1805−1809.
(5) Vispute, T. P.; Zhang, H.; Sanna, A.; Xiao, R.; Huber, G. W. Renewable Chemical Commodity Feedstocks from Integrated Catalytic Processing of Pyrolysis Oils. *Science* **2010**, *330*, 1222−1227.
(6) Carlson, T. R.; Tompsett, G. A.; Conner, W. C.; Huber, G. W. Aromatic Reduction from Catalytic Fast Pyrolysis of Biomass-Derived Feedstocks. *Top. Catal.* **2009**, *52*, 241−252.
(7) Ma, Z.; Troussard, E.; van Bokhoven, J. A. Controlling the Selectivity to Chemicals from Lignin via Catalytic Fast Pyrolysis. *Appl. Catal., A* **2012**, *423*−*424*, 130−136.
(8) Mihalcik, D. J.; Mullen, C. a.; Boateng, A. Screening Acidic Zeolites for Catalytic Fast Pyrolysis of Biomass and its Components. *J. Anal. Appl. Pyrolysis* **2011**, *92*, 224−232.
(9) Zhang, M.; Resende, F. L. P.; Moutsoglou, A.; Raynie, D. E. Pyrolysis of lignin Extracted from Prairie Cordgrass, Aspen, and Kraft Lignin by Py-GC/MS and TGA/FTIR. *J. Anal. Appl. Pyrolysis* **2012**, *98*, 65−71.
(10) Alonso, D. M.; Bond, J. Q.; Dumesic, J. Catalytic Conversion of Biomass to Biofuels. *Green Chem.* **2010**, *12*, 1493−1513.
(11) Demirbas, A. Pyrolysis Mechanism of Biomass Materials. *Energy Sources, Part A* **2009**, *31*, 1186−1193.
(12) Zhao, C.; Lercher, J. A. Upgrading Pyrolysis Oil over Ni/HZSM-5 by Cascade Reactions. *Angew. Chem.* **2012**, *124*, 6037−6042.
(13) Lovell, A. B.; Brezinsky, K.; Glassman, I. The Gas Phase Pyrolysis of Phenol. *Int. J. Chem. Kinet.* **1989**, *21*, 547−560.
(14) Scheer, A. M.; Mukarakate, C.; Robichaud, D. J.; Nimlos, M. R.; Carstensen, H.-H.; Ellison, G. B. Unimolecular Thermal Decomposition of Phenol and d5-Phenol: Direct Observation of Cyclopentadiene Formation via Cyclohexadienone. *J. Chem. Phys.* **2012**, *136*, 044309−044311.
(15) Britt, P. F.; Buchanan, a C.; Cooney, M. J.; Martineau, D. R. Flash Vacuum Pyrolysis of Methoxy Substituted Lignin Model Compounds. *J. Org. Chem.* **2000**, *65*, 1376−1389.
(16) Britt, P. F.; Buchanan, a. C.; Thomas, K. B.; Lee, S.-K. Pyrolysis Mechanisms of Lignin: Surface-Immobilized Model Compound Investigation of Acid-Catalyzed and Free-Radical Reaction Pathways. *J. Anal. Appl. Pyrolysis* **1995**, *33*, 1−19.
(17) Koyama, M. Hydrocracking of Lignin-Related Model Dimers. *Bioresour. Technol.* **1993**, *44*, 209−215.
(18) Maccoll, A. Heterolysis and the Pyrolysis of Alkyl Halides in the Gas Phase. *Chem. Rev.* **1969**, *69*, 33−60.
(19) Kwart, H.; Sarner, S. F.; Slutsky, J. December, R. Mechanism of Thermolytic Fragmentation. *J. Am. Chem. Soc.* **1973**, *95*, 5234−5242.
(20) Klein, M. T.; Virk, P. S. Model Pathways in Lignin Thermolysis; 1. Phenetyl-Phenyl Ether. *Ind. Eng. Chem. Fundam.* **1983**, *22*, 35−45.
(21) Jarvis, M. W.; Daily, J. W.; Carstensen, H.-H.; Dean, A. M.; Sharma, S.; Dayton, D. C.; Robichaud, D. J.; Nimlos, M. R. Direct Detection of Products from the Pyrolysis of 2-Phenethyl Phenyl Ether. *J. Phys. Chem. A* **2011**, *115*, 428.
(22) Beste, A.; Buchanan, A. C. Role of Carbon-Carbon Phenyl Migration in the Pyrolysis Mechanism of β-O-4 Lignin Model Compounds: Phenethyl Phenyl Ether and α-Hydroxy Phenethyl Phenyl Ether. *J. Phys. Chem. A* **2012**, *116*, 12242−12248.
(23) Raff, J. D.; Hites, R. A. Gas-Phase Reactions of Brominated Diphenyl Ethers with OH Radicals. *J. Phys. Chem. A* **2006**, *110*, 10783−10792.
(24) Ouchi, K. Infra-Red Study of Strucutral Changes During the Pyrolysis of a Phenol-Formaldehyde Resin. *Carbon (N.Y.)* **1966**, *4*, 59−66.
(25) Scheer, A. M.; Mukarakate, C.; Robichaud, D. J.; Nimlos, M. R.; Ellison, G. B. Thermal Decomposition Mechanisms of the Methoxyphenols: Formation of Phenol, Cyclopentadienone, Vinylacetylene, and Acetylene. *J. Phys. Chem. A* **2011**, *115*, 13381−13389.
(26) Heitner, C., Dimmel, D., Schmidt, J. *Lignins and Lignans: Advances in Chemistry*; CRS Press: Boca Raton, FL, 2010.
(27) Hemberger, P.; Trevitt, A. J.; Ross, E.; Silva, G. Direct Observation of Para -Xylylene as the Decomposition Product of the Meta-Xylyl Radical Using VUV Synchrotron Radiation. *J. Phys. Chem. Lett.* **2013**, *4*, 2546−2550.
(28) Hemberger, P.; Steinbauer, M.; Schneider, M.; Fischer, I.; Johnson, M.; Bodi, A.; Gerber, T. Photoionization of Three Isomers of the C9H7 Radical. *J. Phys. Chem. A* **2010**, *114*, 4698−4703.

(29) Shin, E.-J.; Nimlos, M. R.; Evans, R. J. The formation of Aromatics from the Gas-Phase Pyrolysis of Stigmasterol: Kinetics. *Fuel* **2001**, *80*, 1689−1687.
(30) Bodi, A.; Hemberger, P.; Gerber, T.; Sztáray, B. A New Double Imaging Velocity Focusing Coincidence Experiment: i2PEPICO. *Rev. Sci. Instrum.* **2012**, *83*, 083105−083108.
(31) Bodi, A.; Johnson, M.; Gerber, T.; Gengeliczki, Z.; Sztáray, B.; Baer, T. Imaging Photoelectron Photoion Coincidence Spectroscopy with Velocity Focusing Electron Optics. *Rev. Sci. Instrum.* **2009**, *80*, 034101−034107.
(32) Johnson, M.; Bodi, A.; Schulz, L.; Gerber, T. Vacuum Ultraviolet Beamline at the Swiss Light Source for Chemical Dynamic Studies. *Nucl. Instrum. Methods Phys. Res., Sect. A* **2009**, *610*, 597−603.
(33) Bodi, A.; Sztáray, B.; Baer, T.; Johnson, M.; Gerber, T. Data Acquisition Schemes for Continuous Two-Particle Time-of-Flight Coincidence Experiments. *Rev. Sci. Instrum.* **2007**, *78*, 084102−084107.
(34) Sztáray, B.; Baer, T. Suppression of Hot Electrons in Threshold Photoelectron Photoion Coincidence Spectroscopy Using Velocity Focusing Optics. *Rev. Sci. Instrum.* **2003**, *74*, 3763−3768.
(35) (a) Frisch, M. J.; Trucks, G. W.; Schlegel, H. B.; Scuseria, G. E.; Robb, M. A.; Cheeseman, J. R.; Scalmani, G.; Barone, V.; Mennucci, B.; Petersson, G. A.; et al.*Gaussian 09*, Revision B.01; Wallingford, CT, 2009. (b) Mozhayskiy, V.; Krylov, A. I. *ezSpectrum*, v 3.0; 2009.
(36) Curtiss, L. A.; Redfern, P. C.; Raghavachari, K. Gaussian-4 Theory Using Reduced Order Pertubation Theory. *J. Chem. Phys.* **2007**, *127*, 124105−124107.
(37) Montgomery, J. A.; Frisch, M. J.; Ochterski, J. W.; Petersson, G. A. A Complete Basis Set model Chemistry. VI. Use of Density Functional Geometrics and Frequencies. *J. Chem. Phys.* **1999**, *110*, 2822−2827.
(38) Vasiliou, A. K.; Piech, K. M.; Reed, B.; Zhang, X.; Nimlos, M. R.; Ahmed, M.; Golan, A.; Kostko, O.; Osborn, D. L.; David, D. E.; et al. Thermal Decomposition of CH3CHO Studied by Matrix Infrared Spectroscopy and Photoionization Mass Spectroscopy. *J. Chem. Phys.* **2012**, *137*, 164308−164318.
(39) Kercher, J. P.; Stevens, W.; Gengeliczki, Z.; Baer, T. Modeling Ionic Unimolecular Dissociation from Temperature Controlled iPEPICO Study on 1-C54H9I Ions. *Int. J. Mass Spectrom.* **2007**, *267*, 159−166.
(40) Sztáray, B.; Bodi, A.; Baer, T. Modeling Unimolecular Reactions in Photoelectron Photoion Coincidence Experiements. *J. Mass Spectrom.* **2010**, *45*, 1233−1245.
(41) Szabo, A.; Barron, L.; August, R. Helium(I) Photoelectron Spectra of Organic Radicals. *J. Am. Chem. Soc.* **1975**, *97*, 662−663.
(42) Patel, P.; Hull, T. R.; McCabe, R. W.; Flath, D.; Grasmeder, J.; Percy, M. Mechanism of Thermal Decomposition of Poly(Ether Ether Ketone) (PEEK) from a Review of Decomposition Studies. *Polym. Degrad. Stab.* **2010**, *95*, 709−718.
(43) Le, H. T.; Flammang, R.; Gerbaux, P.; Bouchoux, G.; Nguyen, M. T. Ionized Phenol and Its Isomers in the Gas Phase. *J. Phys. Chem. A* **2001**, *105*, 11582−92.
(44) Brezinsky, K.; Pecullan, M.; Glassman, I. Pyrolysis and Oxidation of Phenol. *J. Phys. Chem. A* **1998**, *102*, 8614−8619.
(45) Tsai, C. J.; Perng, L. H.; Ling, Y. C. A Study of Thermal Degradation of Poly(Aryl-Ether-Ether-Ketone) Using Stepwise Pyrolysis/Gas Chromatography/Mass Spectrometry. *Rapid Commun. Mass Spectrom.* **1997**, *11*, 1987−1995.
(46) Britt, P. F.; Buchanan, A. C.; Martineau, D. R. *Flash Vacuum Pyrolysis of Lignin Model Compounds: Reaction Pathways of Aromatic Methoxy Groups*; Technical Report CP-101275; Oak Ridge National Laboratory (ORNL): Oak Ridge, TN, 1999, 283−289.
(47) Dorrestijn, E.; Mulder, P. The Radical-Induced Decomposition of 2-Methoxyphenol. *J. Chem. Soc., Perkin Trans. 2* **1999**, *4*, 777−780.
(48) Brigati, G.; Lucarini, M.; Mugnaini, V.; Pedulli, G. F. Determination of the Substituent Effect on the O-H Bond Dissociation Enthalpies of Phenolic Antioxidants by the EPR Radical Equilibration Technique. *J. Org. Chem.* **2002**, *67*, 4828−4832.
(49) Kibet, J.; Khachatryan, L.; Dellinger, B. Molecular Products and Radicals from Pyrolysis of Lignin. *Environ. Sci. Technol.* **2012**, *46*, 12994−13001.
(50) Jegers, H. E.; Klein, M. T. Primary and Secondary Lignin Pyrolysis Reaction Pathways. *Ind. Eng. Chem. Process Des. Dev.* **1985**, *24*, 173−183.
(51) Brebu, M.; Vasile, C. Z Thermal Degradation of Lignin - a review. *Cellul. Chem. Technol.* **2010**, *44*, 353−363.
(52) Nakamura, T.; Kawamoto, H.; Saka, S. Pyrolysis Behavior of Japanese Cedar Wood Lignin Studied with Various Model Dimers. *J. Anal. Appl. Pyrolysis* **2008**, *81*, 173−182.